Int. J. Electrochem. Sci., 9 **(2014)** 3558 - 3573

International Journal of
ELECTROCHEMICAL
SCIENCE
www.electrochemsci.org

Corrosion Behaviour of the Anodic Oxide Film on Commercially Pure Titanium in NaCl Environment

Zuojia Liu[1,*], *Xiaohui Liu*[2], *Uyime. Donatus*[1] , *George. E. Thompson*[1] *and Peter. Skeldon*[1]

[1] Corrosion and Protection Centre, School of Materials, The University of Manchester, M13 9PL, England, UK
[2] Department of equipment safety and corrosion control, SINOPEC Safety Engineering Institute, Qingdao, 266071, China
[*]E-mail: zuojia.liu@gmail.com

Received: 13 March 2014 / *Accepted:* 5 April 2014 / *Published:* 14 April 2014

Anodic oxide growths on commercially pure titanium in 1 M sulphuric and phosphoric acids have been investigated in the present study. Ruptures and blisters of the oxide layers were found as result of a huge pressure of oxygen bubbles developed within the film. The ruptures were more pronounced when higher anodic voltages are reached for both acid anodizations. The oxygen evolution was probably inhibited more significantly for phosphoric acid anodization compared to sulphuric acid anodization. The anodic oxides also showed more ruptures after anodized titanium specimens were immersed for 60 days in naturally aerated 3.5% NaCl electrolyte in higher anodic voltage compared to the immediately ‘just’ immersed conditions in the NaCl electrolyte. The corrosion behaviours of the anodic oxides were studied in the 3.5% NaCl by potentiodynamic polarization and electrochemical impedance spectroscopy. Increased corrosion resistance of the anodic oxides on titanium in NaCl were observed with increase in anodic voltages. The anodic oxide produced in the phosphoric acid showed a higher corrosion resistance than that of the sulphuric acid at each anodizing condition; indicates that the corrosion protection by anodizing for titanium in phosphoric acid should probably be considered in priority compared with sulphuric acid.

Keywords: anodic oxide, titanium, sulphuric acid, phosphoric acid, polarization, impedance

1. INTRODUCTION

In recent decades, titanium has attracted increasing scientific and technological attentions. The combinations of attractive mechanical and chemical properties such as high strength and excellent corrosion resistance have brought a lot of attentions [1-3]. Titanium has been widely used for various ranges of applications such as in aerospace and biological industries [4-7]. Also, more and more chemical industries have considered using titanium materials since the corrosion issues in such plants are as serious as others [8]. It is known that one of the properties of titanium is its immunity to pitting corrosion or stress corrosion cracking in chloride electrolyte which causes corrosion of stainless steels and carbon steels [9]. Consequently, titanium is extensively developed for vessels, heat transfer tubes in steam turbine condensers and multi-stage flashing type desalination plants [9]. However, titanium can still suffer from some corrosion problems such as galvanic corrosion when it is coupled to dissimilar materials in chloride ion containing electrolytes. Titanium differs from most materials in that, if it is coupled to a more noble metal in an aggressive electrolyte, the electrode potential of the titanium tends to decrease and the corrosion rate predicts to increase [10]. Crevice and fretting corrosion are also the main deterioration of titanium material that occurs in the presence of a corrosive medium [9, 11]. As titanium is commonly used in such conditions, corrosion can be a practical serious issue. Thus, surface treatments of titanium were introduced in order to prevent corrosion, and one of the most important techniques which has been developed successfully is anodizing treatments to create a thick anodic oxide film on the metal substrate [12-16].

Titanium oxide films can be created by anodizing treatments in various electrolytes such as sulphuric acid and phosphoric acid. Different oxide properties in terms of thickness, composition or corrosion behaviour are introduced in different anodizing conditions, mainly dependent upon anodic voltage, electrolyte and electrolyte concentration [16-17]. The anodic oxide films are more effective for the promotion of corrosion resistance in critical corrosive environments [15-16]. Recent studies on anodic oxide growth of titanium have been documented at a certain degree, and some interesting phenomenons were found. Anodic titania performs an amorphous-to-crystalline transition at voltages as low as ~ 10 V [18]. Oxygen evolution was recorded during titanium anodic oxide growth because crystallization resulted in high electronic conductivity. The oxygen gas bubbles generated at the crystalline regions increased gas pressure in the bubbles with film growth resulting in the breakdown of the anodic film [19]. It is investigated the corrosion resistance of titanium can be improved by anodic oxide films fabricated in phosphate buffer media for the bio-corrosive environment [20]. Anodic oxidative film of titanium is also reported to lower the corrosion rate in chlorinated working environments such as hazardous waste water industries [21].

Further, it has been proved that titanium exhibits markedly resistance to corrosion in neutral chloride environments even at relatively high temperatures. However, the anodic oxide of titanium is still probably influenced by chloride and oxygen ions in the electrolyte. The effects which might be caused by the integration between oxygen and chlorides for the destructive behaviour of anodic oxide of titanium are still not clear. Also, the comparison between the corrosion resistance of titanium anodic oxide formed in sulphuric acid and the oxide produced in phosphoric acid, in chlorides containing environments has not been fully understood. Thus, in the present paper, the anodic oxide growth of titanium in sulphuric and phosphoric acids, respectively were studied and electrochemical corrosion behaviour of the anodic oxide on titanium was investigated in NaCl electrolyte following anodizing under different conditions. Potentiodynamic polarization and electrochemical impedance spectroscopy measurements were monitored in naturally aerated NaCl environment. The morphology of relative anodic oxide films were complemented by scanning electron microscopy.

2. EXPERIMENTAL PROCEDURES

2.1. Material and anodizing treatments

Titanium specimens of 3.0 ×1.5 cm^2 area were obtained from grade II commercially pure titanium (cp-Ti) sheet of 1.0 mm thickness and masked by beeswax to define an exposing area of 1.0 cm^2 for the anodizing and electrochemical test electrolytes. The composition of titanium sample in percent weight contains Fe, 0.03-0.20; H, 0.001-0.015; O, 0.04-0.18; N, 0.01-0.03; C, 0.01-0.08; Ti, bal. In order to remove the contaminants, the titanium materials were etched in Kroll's reagent (5% HNO_3 + 10% HF + 85% distilled H_2O) for 15 s at ambient temperature [22]. Before anodic treatment, the titanium specimens were cleaned in acetone, rinsed in de-ionized water and dried in a cool air stream. The anodizing treatments employed two-electrode cell, with an aluminium sheet as the counter electrode. The anodizing tests were carried out galvanostatically at 20 mA cm^{-2} in 1 M phosphoric acid and 1 M sulphuric acid electrolytes to 20, 40 and 60 V, respectively. The voltage variation was recorded by a computer interfaced with the laboratory DC power supply at 293 K. Following anodizing, the specimens were removed from the electrolyte, cleaned in de-ionized water, dried in a cool air stream and stored in a desiccator until required for further analysis. Selected specimens after anodizing were immersed in the naturally aerated 3.5% NaCl electrolyte for 60 days.

2.2. Electrochemical measurements

Electrochemical experiments were performed in the aqueous 3.5% NaCl electrolyte at 293 K, using a Solartron Analytical Modulab System. A conventional three-electrode system with the cp-Titanium as working electrode, and a platinum auxiliary electrode and a saturated calomel reference electrode (SCE) was employed. Polarisation measurements of the titanium specimens at each anodizing condition were investigated under potentiodynamic regulation over the potential range from -1.0 V (SCE) to 6.0 V (SCE) at a scan rate of 1.0 mV s^{-1} in order to probe the respective anodic and cathodic behaviours. Electrochemical impedance spectroscopy measurements were carried out in potentiostatic mode and vs. open circuit, with voltage perturbation amplitude of 10 mV with 10 points per decade without start delay, in the frequency range from 100 kHz to 0.01 Hz. The tests were also employing the Solartron workstation using the same three-cell arrangement. The impedance results were analyzed by using ZSim software. All electrochemical curves were plotted by origin 9.0 program. The potentiodynamic polarization and electrochemical impedance spectroscopy measurements were conducted on the etched specimen immediately immersed and the specimens after the anodizing processes of the sulphuric and phosphoric acids in the neutral 3.5% NaCl separately. The electrochemical measurements were also carried out on the etched and anodized specimen after immersion in the 3.5% NaCl electrolyte for 60 days. Prior to all electrochemical experiments, the working electrode was held in the sodium chloride electrolyte for 30 min to approach a stable potential by applying the test of open circuit (SCE).

2.3. Morphology characterization

The original titanium specimen after etching in the Kroll's reagent, the anodic oxide films produced to 20, 40 and 60 V in 1 M sulphuric and 1 M phosphoric acids respectively, and the etched and all anodized titanium specimens after immersion in the 3.5% NaCl for 60 days were examined by scanning electron microscopy (SEM) instrument of Zeiss Ultra 55, with the acceleration voltage of 5 kV in a high vacuum environment.

3. RESULTS AND DISCUSSION

3.1. Voltage-time responses

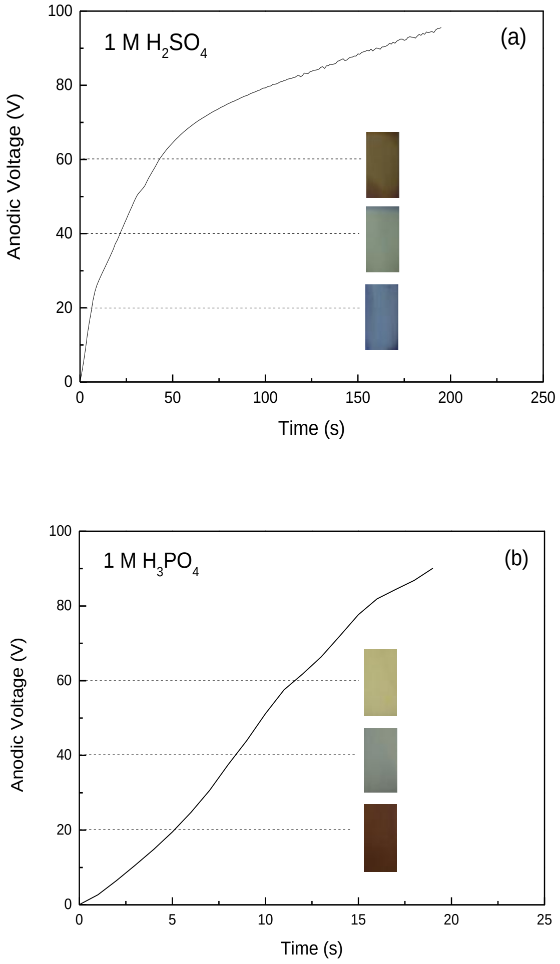

Figure 1. Voltage-time responses of the anodizing process of cp-Ti in 1 M H_2SO_4 (a) and H_3PO_4 (b) electrolytes at 20 mA cm^{-2}, respectively at 293 K.

The voltage-time response for titanium anodized at 20 mA cm^{-2} in 1 M H_2SO_4 resulted in an initial surge to about 2 V due to pre-existed air-formed oxide (Figure 1a). A relatively rapid rise to an approximate voltage of about 26 V was attained at 3.2 V s^{-1}. The rise slowed slightly from nearly 26 V to 60 V followed by a significant reduction of the rise for the rest of the duration, and the anodizing was terminated at around 97 V. The colour scales vary from sky blue-pale blue-dark yellow with anodic voltages of 20, 40 and 60 V due to interference effect [23]. Anodizing of titanium at 20 mA cm^{-2} in 1 M H_3PO_4 revealed an initial surge to about 3 V, attributable to a pre-existing air-formed oxide, followed by an approximately linear rise at about 4 V s^{-1} (Figure 1b). The rise then slightly accelerated to an average value in the range of 4.2-4.4 V s^{-1} for about 7 s to 11 s. The rise slowed to around 90 V at 18 s that the anodizing was terminated. Figure 1b also displays different surface colours of titanium after the anodizing processes. The colour variations of the anodized titanium specimens in 1 M H_3PO_4 are scaled from brown-pale blue-pale yellow with respect to 20, 40 and 60 V, respectively. The time of anodic oxide growth for titanium in H_3PO_4 is much shorter to reach 20, 40 and 60 V, respectively compared to H_2SO_4, showing a higher current efficiency for oxide growth from H_3PO_4 anodization. Further, oxygen bubbles attached to the titanium surface were visible by naked eyes during all anodizing tests, confirming the occurrence of oxygen evolution.

3.2. Scanning electron microscopy characterization

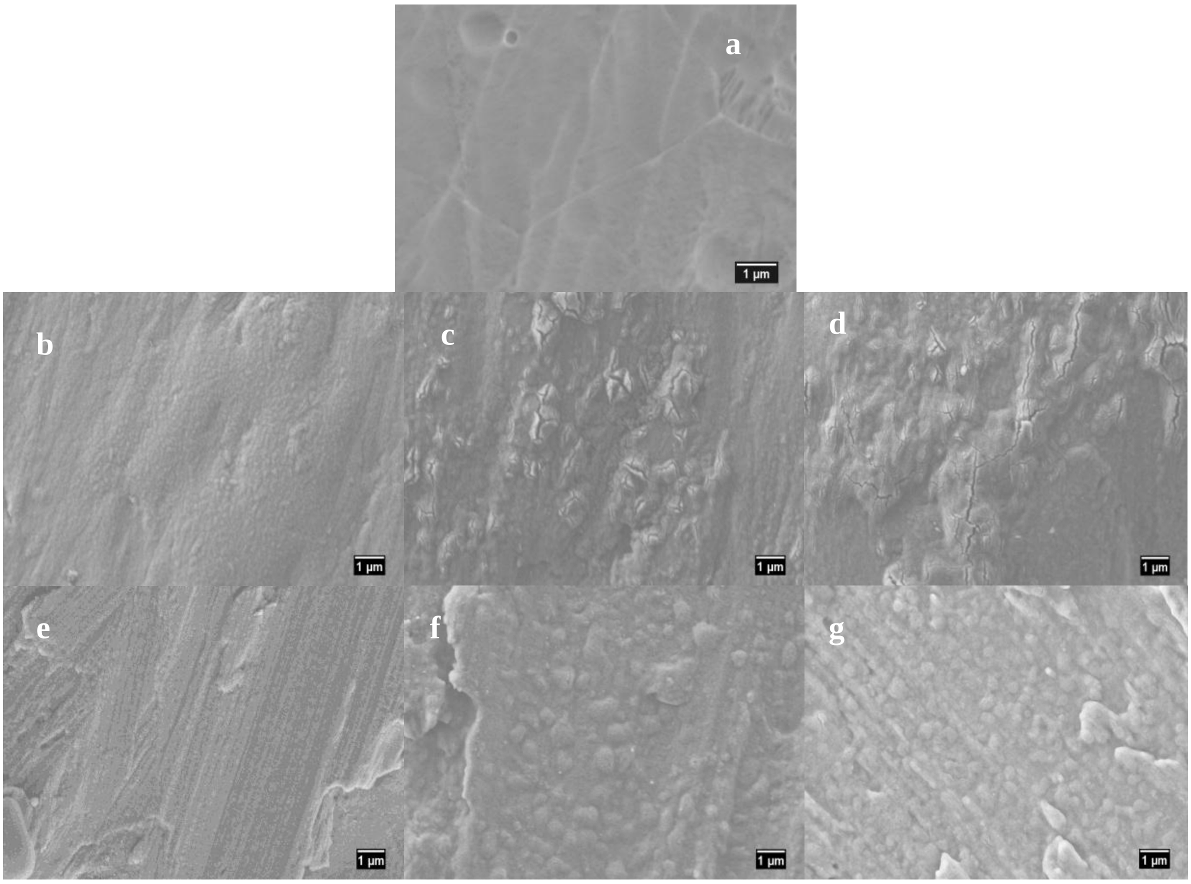

Figure 2. Scanning electron micrographs of etched titanium, and the anodic oxides formed on titanium at 20 mA cm^{-2} for different conditions in 1 M H_2SO_4 and H_3PO_4 electrolytes, respectively at 293 K: (a) original titanium after etching in Kroll's reagent; anodizing in H_2SO_4 to (b) 20 V, (c) 40 V and (d) 60 V; anodizing in H_3PO_4: (e) 20 V, (f) 40 V and (g) 60 V.

Figure 2 shows the morphology of the etched titanium and the oxide layers formed by anodizing to different anodic voltages in sulphuric and phosphoric acids that were selected for detailed analyses using scanning electron microscopy. Figure 2a shows the titanium after etching in the Kroll's electrolyte, revealing the grain boundaries across the surface of titanium. Figure 2b indicates the mainly amorphous oxide showing a compact structure formed by anodizing when 20 V was reached in the sulphuric acid electrolyte. Figure 2c displays the oxide ruptures locally due to sufficient oxygen evolution occurring during anodization to 40 V. The oxide ruptures with introduction of cracks were observed at an anodic voltage of 60 V (Figure 2d). In accordance with phosphoric acid anodizing, the main amorphous oxide is revealed at an anodic voltage of 20 V (Figure 2e). The blister textures are evident as bubbles to be initiated at the voltage of 40 V (Figure 2f). Similar oxide layer with local pluck up oxygen bubble is present when anodized to 60 V, as shown in Figure 2g.

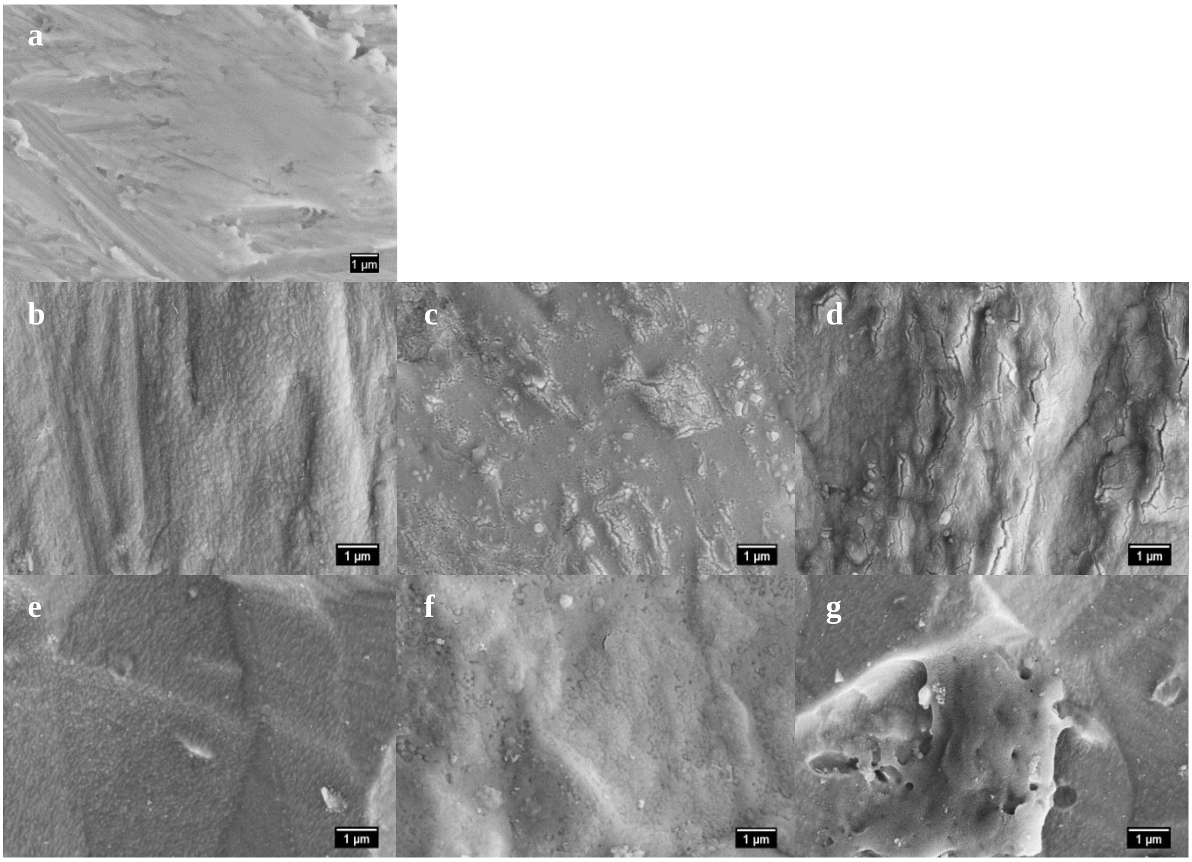

Figure 3. Scanning electron micrographs of titanium after etching in Kroll's reagent, and anodized titanium at 20 mA cm^{-2} for different conditions in 1 M H_2SO_4 and H_3PO_4 electrolytes, respectively after immersion for 60 days in naturally aerated 3.5% NaCl electrolyte at 293 K; (a) original etched titanium; anodized in H_2SO_4 to (b) 20 V, (c) 40 V and (d) 60 V; anodized in H_3PO_4: (e) 20 V, (f) 40 V and (g) 60 V.

The micrographs of the etched titanium and the anodic oxide surfaces after immersion in naturally aerated 3.5% NaCl electrolyte for 60 days at room temperature are shown in Figure 3. The SEM micrograph clearly shows that the metal surface is covered by a thin passive oxide formed from oxygen in the NaCl electrolyte (Figure 3a). Figure 3b shows that the oxide formed by the sulphuric acid anodizing to 20 V followed by the immersion in naturally aerated 3.5% NaCl electrolyte is less uniform compared to anodized surface without immersion in naturally aerated 3.5% NaCl electrolyte., and some small oxygen bubbles are observed. It is revealed that the oxide surface is insignificantly different from the morphology obtained after the anodizing procedures only, except that the rupture of oxide is more significant when 40 and 60 V were reached in this case (Figure 3c and d). One of the possibilities is that the anodic oxides were attacked by the chloride ions at a small degree, resulting in the extension of rupture [24]. Figure 3e shows that the oxide formed to 20 V in the phosphoric acid contains nano-oxygen bubbles which probably lead the surface to be less uniform compared to the anodized surface. Figure 3f displays the oxide surface formed to 40 V in the H_3PO_4 electrolyte is occupied by a uniform region and a localized rupture, the bubble textures are not appearing in contrast to the anodized specimen without immersion. Figure 3g shows that the oxide microstructure produced to 60 V with localized pores developed due to probably the dissolution of the bubbles found in the previous anodizing case.

Comparison between the two acid electrolytes is gained by the SEM observations, the impacts from oxygen bubbles developed within the oxide produced via sulphuric acid probably starts earlier than the phosphoric acid electrolyte among the anodic voltages selected. Greater inhibition of oxygen evolution during the anodic oxide growth on titanium in phosphoric acid can be assumed in comparison with sulphuric acid. It has been reported that oxide amorphous-to-crystalline transition cannot be ruled out for the growth of titanium anodic oxide [18]. The oxygen bubbles generated from oxygen evolution are developed within the crystalline phase due to its higher electron-conducting behaviour compared to the adjacent amorphous phase [19], this allows ingress of the electrolyte in proximity to the metal-oxide interface, resulting in rupture. When the anodic voltage increases, more current efficiencies for the oxide growth will be consumed by oxygen evolution, thus, the textures containing oxygen bubbles are more significant, and the correspondent cracking textures can be observed. After the immersion experiments in the 3.5% NaCl electrolyte, the defects of anodic oxides are revealed more seriously, indicating that the dissolution of the film could be induced by the development of oxygen bubbles and attack of chloride ions. It is also clarified that according to point defect model [25], the oxide contains oxygen vacancies which is taken place at the interface oxide / electrolyte, and the chloride ions would be absorbed in and react with the vacancies, thereby, introducing more metal vacancies. Further, the redundant metal vacancies locate in the interface metal / oxide, leading to the rupture of oxide [26].

3.3. Electrochemical impedance spectroscopy

The original titanium after etching and the immersed condition in 3.5% NaCl electrolyte were investigated by the impedance spectra, plotted by Bode diagrams (Figure 4). Slightly higher impedance was measured for the etched titanium compared to the immersed etched specimen in NaCl for 60 days. The capacitive behaviour from medium to low frequencies is more significant with phase shift approaching -90° on the immersed titanium in NaCl than the just etched specimen due to the removal of air-formed film by etching.

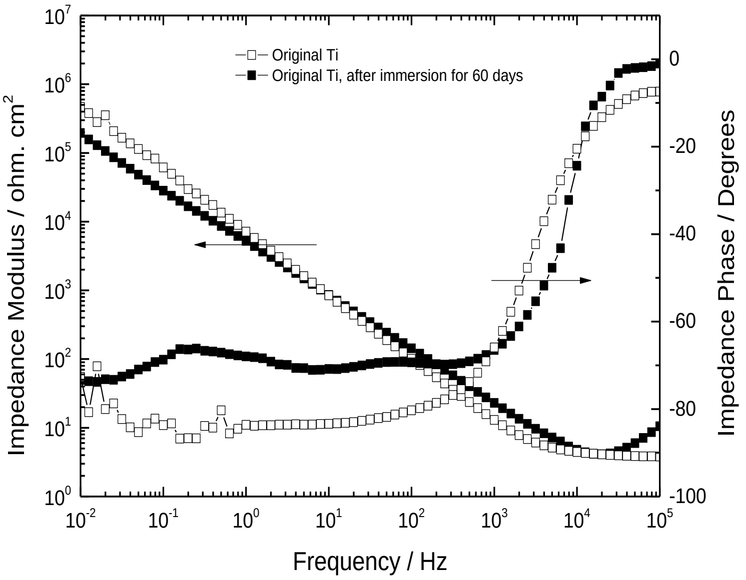

Figure 4. Bode plots of the original titanium before immersion and after immersion for 60 days in naturally aerated 3.5% NaCl electrolyte at 293 K.

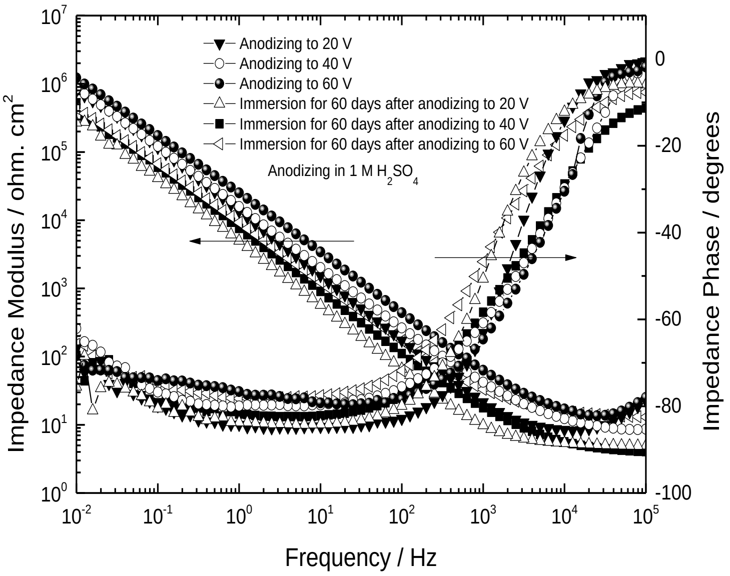

Figure 5. Bode plots of titanium oxides in 1 M H_2SO_4 to 20, 40 and 60 V, respectively, and immersion for 60 days in naturally aerated 3.5% NaCl electrolyte after the anodizing treatments.

The typical appearance of the impedance spectra as a function of the applied potential at which the impedance was measured is presented in Figure 5 and Figure 6 for the anodized titanium in the H_2SO_4 and H_3PO_4 electrolytes, respectively. Over the frequency range, the impedance for the anodized titanium in both acids increases slightly with increase in anodic voltage, suggesting a reduced capacitance of the anodic film.

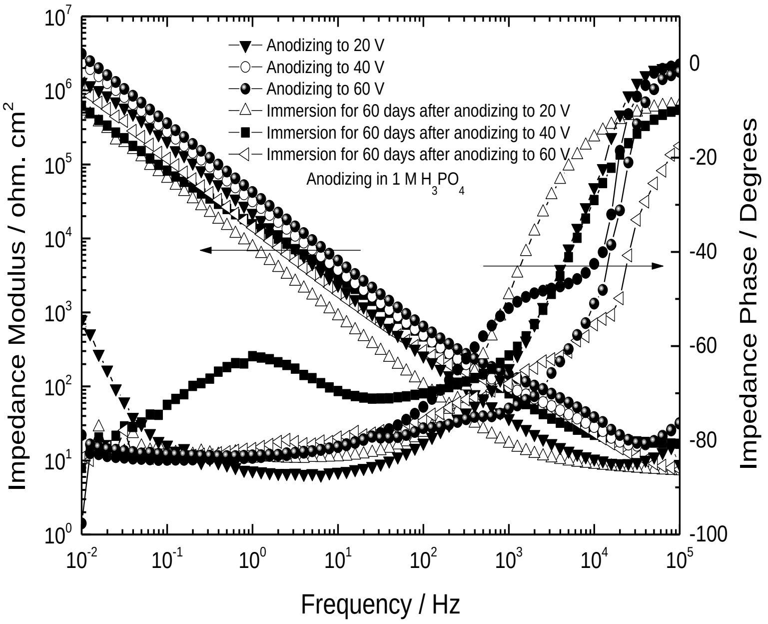

Figure 6. Bode plots of titanium oxides in 1 M H_3PO_4 to 20, 40 and 60 V, respectively, and immersion for 60 days in naturally aerated 3.5% NaCl electrolyte after the anodizing treatments.

The anodized titanium after immersion in 3.5% NaCl electrolyte reveals increased impedance with anodic voltage increases, and the impedances are more negative than the anodized titanium specimens without immersion in NaCl at each relative anodizing condition. Furthermore, as the frequency window is inspected, one time constant is observed since all impedances change approximately linearly with frequency, with a slope of -1. A predominantly capacitive behaviour is evident, indicating from medium to low frequencies by the phase shifts approaching -90^o, suggesting that a highly stable oxide film is formed on titanium in both acids during the anodizing to 20, 40 and 60 V, separately. After immersion in NaCl for the duration of 60 days, the oxide capacitive field is reduced by lowering the phase shifts to approach -80^o from the medium to low frequencies.

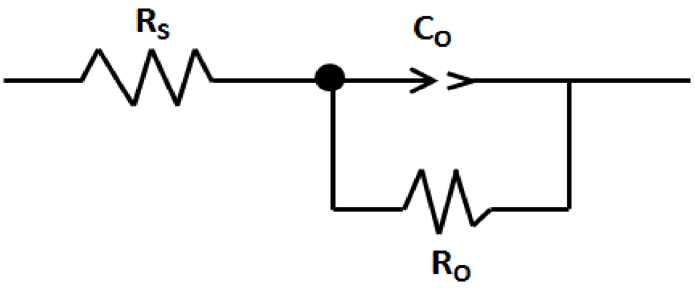

Figure 7. Equivalent circuit proposed to model the impedance spectra. R_s, C_o, R_o, electrolyte resistance, oxide capacitance and resistance associated with current flow across the oxide.

The parameters were fitted by using an R(CR) circuit consisting of a capacitor, accounting for the capacitive behaviour of the anodic film, in parallel with a resistor, being responsible for the dissipative resistance to current flow across the oxide, both in series with a resistor accounting for the electrolyte resistance (Figure 7). The results are listed in Table 2. It is shown that the oxide impedance resistance increases with an increase in anodic voltage in terms of 'just' anodizing in both acids and immersion in NaCl after anodizing conditions, respectively, indicating increased corrosion resistance in the NaCl electrolyte by reaching more positive anodic voltages. The oxide capacitance is decreased with the increase in anodic voltage before and after the immersion situations, resulting in a high electric field developed across the anodic oxide due to the amorphous-to-crystalline transition [27]. The oxide capacitance characterizes the relationship with the oxide thickness, as expressed by the following equation:

$$C = \frac{\varepsilon_0 \varepsilon_r A}{d} \tag{1}$$

Where Eq. (1) shows that the capacitance C is a function of the absolute permittivity in vacuum ε_0 (8.85×10^{-12} F m^{-1}), the relative permittivity of TiO_2 ε_r (the value of 80 is assumed [28-29] the area A of the capacitor (1.0 cm^2) and the oxide thickness d.

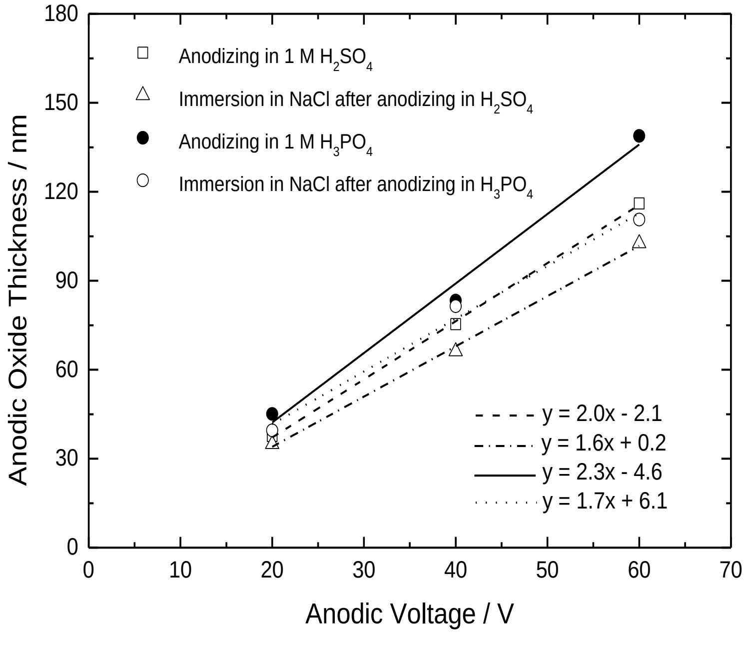

Figure 8. The oxide thickness as a function of anodic voltage before and after immersion experiments in naturally aerated 3.5% NaCl electrolyte, respectively.

Figure 8 shows the anodic oxide thickness is linear functioned with anodic voltage in all circumstances. It deduces a film growth rate, for the titanium, of 2.0 nm V^{-1} after anodizing in H_2SO_4 and 2.3 nm V^{-1} in H_3PO_4 electrolyte. The 60 days immersion in 3.5% NaCl yields a growth rate, for the anodized titanium in H_2SO_4, of 1.6 nm V^{-1} and 1.7 nm V^{-1} in H_3PO_4. During the immersion tests in NaCl electrolyte for 60 days, the re-growth of anodic oxide is probably induced by vigorous oxygen contents, maintaining the film thickness, as estimated by electrochemical impedance spectroscopy in this case. Thus, in comparison with sulphuric acid, the anodizing prepared in the phosphoric acid at the same condition can attract a thicker anodic oxide film and a better corrosion resistance in the NaCl environment. Thus, for the critical and crucial working environment containing Cl^-, the anodizing carried out in phosphoric acid should probably be considered in priority rather than in sulphuric acid in order to provide surface protection for the commercially pure titanium.

Table 1. The electrochemical impedance spectroscopy parameters of cp-Ti electrode in different experimental conditions.

Experimental Condition	Anodic Voltage (V)	R_s (Ω.cm^2)	R_o (Ω.cm^2)	C_o (μF cm^{-2})
Etched in Kroll's reagent	/	9.07	7.57×10^3	0.92
Immersed in NaCl	/	8.198	2.22×10^6	10.92
1 M H2SO4	20	8.405	4.33×10^6	1.88
	40	9.057	8.99×10^6	0.94
	60	13.68	11.15×10^6	0.61
Immersed in NaCl after anodizing in H_2SO_4	20	10.62	1.13×10^6	2.03
	40	10.28	3.16×10^6	1.07
	60	12.93	7.36×10^6	0.69
1 M H_3PO_4	20	12.75	6.49×10^6	1.57
	40	12.92	1.30×10^7	0.85
	60	13.81	6.93×10^7	0.51
Immersed in NaCl after anodizing in H_3PO_4	20	15.60	3.59×10^6	1.79
	40	11.09	6.76×10^6	0.87
	60	11.99	8.17×10^6	0.64

3.4. Potentiodynamic polarization measurements

The potentiodynamic polarization curve of the original titanium after etching in Kroll's reagent shows that a narrow passive region initiates from -0.62 V (SCE) to about 0 V (SCE), followed by an curve shifting the current to increase due to the occurrence of oxygen evolution, until the potential reaches around 1.50 V (SCE), and a later secondary passivation region to 6 V (SCE) (Figure 9). The potentiodynamic polarization curve obtained for the etched titanium after immersion in 3.5% NaCl electrolyte for 60 days (Figure 9) shows similar passive-O_2 evolution transition, starts from -0.35 V (SCE) to 1.80 V (SCE), and secondary passive state is maintained until 6 V (SCE). The corrosion potentials and corrosion current densities were obtained from the polarization curves via Tafel method [30] and are listed in Table 2, which indicates that the corrosion potential and corrosion current density for the titanium after etching are both lower than the 60 days immersed titanium in NaCl electrolyte.

Figure 10 shows the potentiodynamic polarization curves for anodized titanium to 20, 40 and 60 V respectively in 1 M H_2SO_4 'just' immersed and immersed for 60 days in naturally aerated NaCl electrolyte. Common features including the evidence of a passive region in all the conditions, starting from almost -0.60 V (SCE), and a decline in current density from each relatively passive state, indicative of passivity between approximately -0.50 V (SCE) and 0.60 V (SCE), are evident. The oxygen evolution is triggered after the passive region, and maintained until the secondary-passive state occurs from about 3.10 V (SCE), leading to a rise in current density.

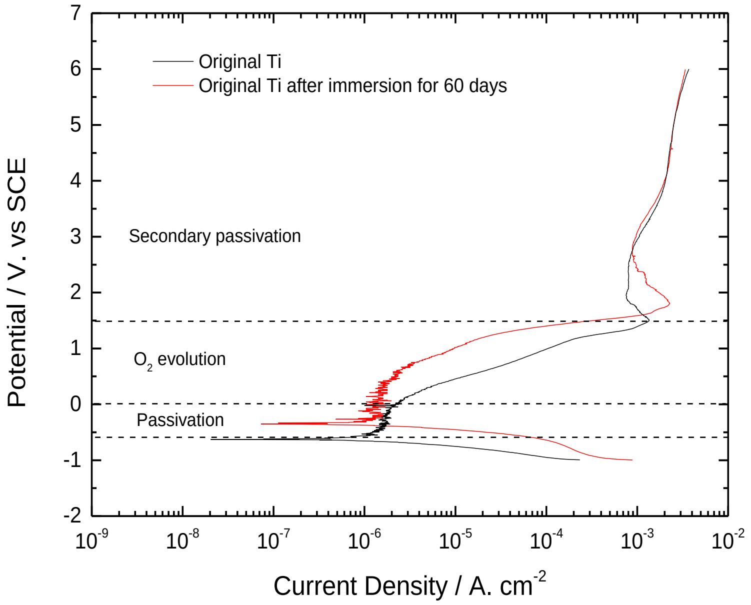

Figure 9. Potentiodynamic polarization curves of the original titanium immediately immersed and after immersed for 60 days in naturally aerated 3.5% NaCl electrolyte at 293 K.

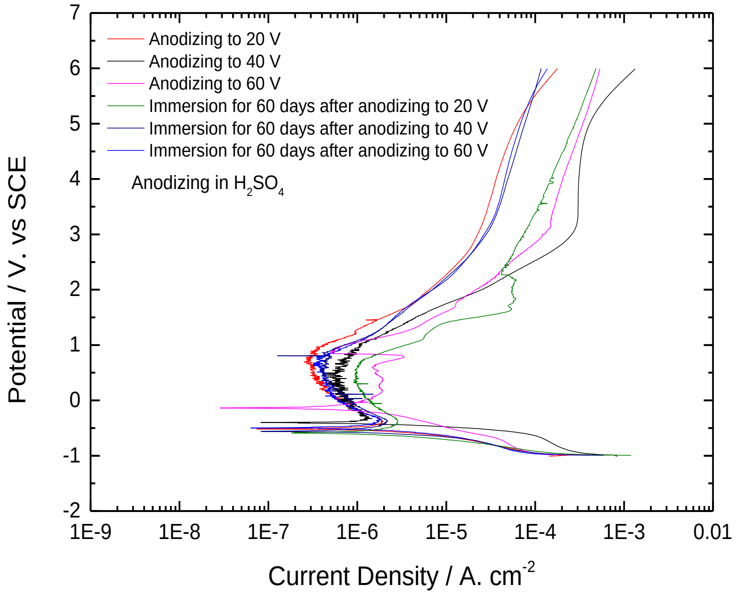

Figure 10. Potentiodynamic polarization curves of the anodized titanium in 1 M H_2SO_4 immediately immersed and immersed for 60 days in naturally aerated 3.5% NaCl electrolyte at 293 K.

The potentiodynamic polarization plots of the anodized titanium to 20, 40 and 60 V respectively in 1 M H_3PO_4 ‘just’ immersed and immersed for 60 days in naturally aerated NaCl electrolyte after the anodizing processes are presented in Figure 11. It is revealed a passive region in all the situations starts from around -0.5 V (SCE). By increasing the potential from the corrosion potential within the passive region, the current density decreases slightly due to the formation of protective passive film. The current density increases rapidly after the passive state due to oxygen evolution until secondary-passivated polarization dominates after a potential of about 3.21 V (SCE).

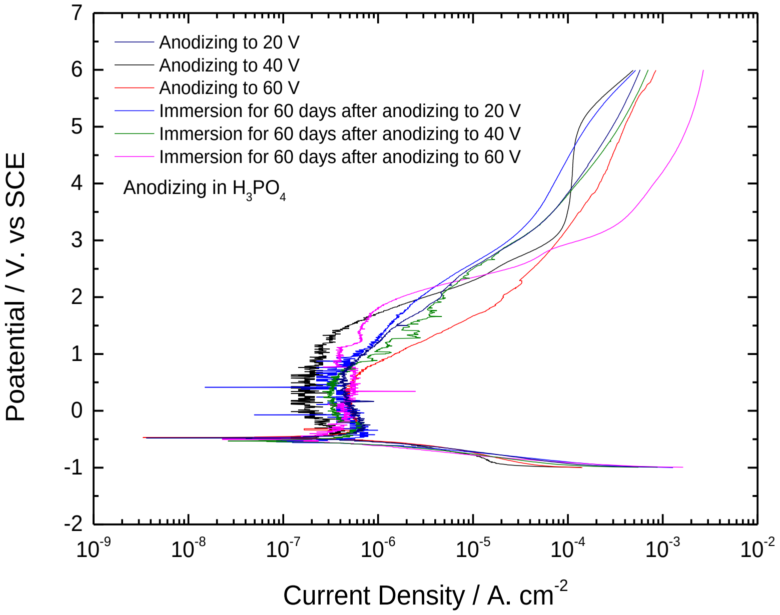

Figure 11. Potentiodynamic polarization curves of the anodized titanium in 1 M H_3PO_4 immediately immersed and immersed for 60 days in naturally aerated 3.5% NaCl electrolyte at 293 K.

The relative corrosion potentials and corrosion current densities are listed in Table 2. Compared to the originally etched titanium, the corrosion potentials for the anodized specimens become more positive but corrosion current densities become lower. The corrosion potential of the anodized titanium increases slightly with increase in anodic voltage, while the current density decreases. Similar results are also revealed for the immersed titanium in 3.5% NaCl after anodizing in the H_2SO_4 and H_3PO_4 electrolytes respectively, indicating a similar trend that increased anodic voltage results in the increase of corrosion potential slightly and more negative corrosion current density. The corrosion rate is determined by the corrosion current density [31], higher current density signals higher corrosion rate during polarization measurement. Thus, the dissolution rate of the anodic oxide films may grow with higher corrosion current density. However, the oxygen bubbles developed within the anodic oxide film previously after ‘just’ anodizing in H_2SO_4 and H_3PO_4 electrolytes, respectively, introduce a huge pressure for the film to be dissolved. Consequently, after the immersion treatments in NaCl electrolyte for 60 days, the oxide films are further ruptured in localized regions by the development of oxygen evolution and invasion of chloride ions [26]. Additionally, the incorporation of phosphate species into the anodic oxide films during anodizing in the phosphoric acid electrolyte impedes an amorphous-to-crystalline transition to a more degree compared to the sulphate species from the sulphuric acid electrolyte [32]. Therefore, the existence of phosphate species leads the corrosion potentials to be more positive and current densities to be lower in the neutral aerated 3.5% NaCl electrolyte in comparison with the sulphate species.

Table 2. The potentiodynamic polarization parameters of cp-Ti electrode in different experimental conditions.

Experimental Condition	Anodic Voltage (V)	Corrosion Potential (V. vs SCE)	Corrosion Current Density (A. cm^{-2})
Etched in Kroll's reagent	/	-0.62	8.50×10^{-7}
Immersed in NaCl	/	-0.35	9.64×10^{-7}
1 M H_2SO_4	20	-0.51	5.71×10^{-7}
	40	-0.40	5.39×10^{-7}
	60	-0.14	3.78×10^{-7}
Immersed in NaCl after anodizing in H_2SO_4	20	-0.59	6.69×10^{-7}
	40	-0.56	6.06×10^{-7}
	60	-0.50	5.77×10^{-7}
1 M H_3PO_4	20	-0.48	1.29×10^{-7}
	40	-0.48	1.12×10^{-7}
	60	-0.47	7.45×10^{-8}
Immersed in NaCl after anodizing in H_3PO_4	20	-0.54	2.15×10^{-7}
	40	-0.53	1.64×10^{-7}
	60	-0.50	1.21×10^{-7}

4. CONCLUSIONS

The anodic oxide growth of commercially pure titanium in sulphuric and phosphoric acids was investigated by scanning electron microscopy observations. The morphology showed oxide rupture due to oxygen bubbles formed from oxygen evolution during anodizing within the anodic oxide, this exerts a lot of pressure within the film and a consequent blister surface texture. The oxide rupture is more serious when it is produced in 1 M sulphuric acid than 1 M phosphoric acid, indicating that oxygen evolution is probably impeded more in the phosphoric acid. It was also observed that the anodic oxides showed more rupture after anodized titanium were immersed for 60 days in naturally aerated 3.5% NaCl in higher anodic voltages, compared to the immediately 'just' immersed conditions. The corrosion behaviour of the anodic oxides at different conditions was studied by podentiodynamic polarization and electrochemical impedance spectroscopy for the conditions of 'just' immersed and immersed for 60 days in 3.5% NaCl electrolyte. The results showed that the corrosion resistance for commercially pure titanium can be improved against attack of chlorides by anodizing treatments, and the corrosion resistance increases with increase in anodic voltage. The anodic oxide formed in the phosphoric acid can provide a higher corrosion resistance than that of the sulphuric acid at the same anodizing condition, thus, the corrosion protection by using anodizing for titanium carried out in phosphoric acid should be probably considered in priority ahead of sulphuric acid in critical chlorides containing environments.

ACKNOWLEDGMENTS
The present work was carried out in Corrosion and Protection Centre, School of Materials, The University of Manchester. The authors thank EPSRC (Engineering and Physical Science Research Council, UK) for financial support in the development of this research.

References

1. J. C. M. Souza, S. L. Barbosa, E. Ariza, J. P. Celis, L. A. Rocha, *Wear.,* 292 (2012) 82 .
2. M. V. Diamanti *et al., Surf. Coat. Technol.,* 227 (2013) 19.
3. C. Fei, Z. Hai, C. Chen, X. Yangjian, *Prog. Org. Coat.,* 64 (2009) 264.
4. L. Mohan, C. Anandan, *Appl. Surf. Sci.,* 282 (2013) 281.
5. A. R. Shankar, N. S. Karthiselva, U. K. Mudali, *Surf. Coat. Technol.,* 235 (2013) 45.
6. N. Schiff, B. Grosgogeat, M. Lissac, F. Dalard, *Biomaterials.,* 23 (2002) 1995.
7. L. Reclaru, J. M. Meyer, *Biomaterials.,* 19 (1998) 85.
8. R. W. Schutz, H. B. Watkins, *Mater. Sci. Eng., A.,* 243 (1998) 305.
9. K. S. a. F. K. H. Satoh, *Platinum Metals.,* 31 (1987) 115.
10. R. W. R. a. H. H. Uhlig. (John Wiley & Sons, Inc, New Jersey, 2008).
11. S. Kumar, T. S. N. S. Narayanan, S. Ganesh Sundara Raman, S. K. Seshadri, *Mater. Sci. Eng., C.,* 30 (2010) 921.
12. H.-J. Song, M.-K. Kim, G.-C. Jung, M.-S. Vang, Y.-J. Park, *Surf. Coat. Technol.,* 201 (2007) 8738.
13. Y. Wang, T. Lei, B. Jiang, L. Guo, *Appl. Surf. Sci.,* 233 (2004) 258.
14. P. S. Gordienko *et al., Prot. Met.,* 44 (2008) 475.
15. A. K. Sharma, *Thin Solid Films.,* 208 (1992) 48.
16. H. Badekas, C. Panagopoulos, *Surf. Coat. Technol.,* 31 (1987) 381.
17. M. P. Q. Cui, O. K. Varghese and C. A. Grimes, *J. Mater. Res.,* 20 (2005) 230.
18. H. Habazaki *et al., Corros. Sci.,* 45 (2003) 2063.
19. M. T. Tanvir *et al., Electrochim. Acta.,* 52 (2007) 6834.
20. I. S. P. Madhav Prasad Neupane, Sook Jeong Lee, Kyoung A Kim, Min Ho Lee, Tae Sung Bae, *Int. J. Electrochem. Sci.,* 4 (2009) 197.
21. N. E. D.B. Mitton, J.A Cline, and R.M. Latanision, *Technology Reviews & Studies.,* 16 (2001) 30.
22. L. Pazos, P. Corengia, H. Svoboda, *J. Mechanical Behavior Biomedical Materials.,* 3 (2010) 416.
23. S. Van Gils, P. Mast, E. Stijns, H. Terryn, *Surf. Coat. Technol.,*185 (2004) 303.
24. M. Atapour, A. L. Pilchak, M. Shamanian, M. H. Fathi, *Mater & Des.,* 32 (2011) 1692.
25. D. D. Macdonald, *Electrochim. Acta.,* 56 (2011) 1761.
26. R. Narayanan, S. K. Seshadri, *Corros. Sci.,* 50 (2008) 1521.
27. A. Mazzarolo, M. Curioni, A. Vicenzo, P. Skeldon, G. E. Thompson, *Electrochim. Acta.,* 75 (2012) 288.
28. J. Li, S. J. Li, Y. L. Hao, R. Yang, *Int. J. Hydrogen Energy.,* In Press (2014) 1.
29. J. Robertson, *EPJ. Appl. Phys.,* 28 (2004) 265.
30. E. McCafferty, *Corros. Sci.,* 47 (2005) 3202.
31. W. A. G. Rabab M. Abou Shahba, Azza El-Sayed El-Shenawy, Amal S. I. Ahmed and Safaa M. Tantawy, *Int. J. Electrochem. Sci.,* 6 (2011) 5499.

32. H. Habazaki, M. Teraoka, Y. Aoki, P. Skeldon, G. E. Thompson, *Electrochim. Acta.*, 55 (2010) 3939.